

Superposition Violations in the Compensatory Eye Movement System

Tafadzwa M. Sibindi,^{1,2} Peter J. Holland,^{1,2} Jos N. van der Geest,¹ Opher Donchin,^{1,2} and Maarten A. Frens^{1,3}

¹Department of Neuroscience, Erasmus University Medical Center, Rotterdam, The Netherlands

²Department of Biomedical Engineering, Ben-Gurion University of the Negev, Beer-Sheva, Israel

³Erasmus University College, Rotterdam, The Netherlands

Correspondence: Maarten A. Frens, Department of Neuroscience, Erasmus University Medical Center, Wytemaweg 80, 3015 CN Rotterdam, The Netherlands; m.frens@erasmusmc.nl.

Submitted: November 17, 2015
Accepted: April 16, 2016

Citation: Sibindi TM, Holland PJ, van der Geest JN, Donchin O, Frens MA. Superposition violations in the compensatory eye movement system. *Invest Ophthalmol Vis Sci*. 2016;57:3554–3566. DOI:10.1167/iov.15-18605

PURPOSE. Compensatory eye movements (CEM) maintain a stable image on the retina by minimizing retinal slip. The optokinetic reflex (OKR) and vestibulo-ocular reflex (VOR) compensate for low and high velocity stimuli, respectively. The OKR system is known to be highly nonlinear. The VOR is generally modeled as a linear system and assumed to satisfy the superposition and homogeneity principles. To probe CEM violation of the superposition principle, we recorded eye movement responses in C57BL/6 mice to sum of sine (SoS) stimulation, a combination of multiple nonharmonic inputs.

METHODS. We tested the VOR, OKR, VVOR (visually enhanced VOR), and SVOR (suppressed VOR). We used stimuli containing 0.6 Hz, 0.8 Hz, 1.0 Hz, and 1.9 Hz. Power spectra of SoS stimuli did not yield distortion products. Gains and delays of SoS and single sine (SS) responses were compared to yield relative gains and delays.

RESULTS. We find the superposition principle is violated primarily in the OKR, VOR, and SVOR conditions. In OKR, we observed relative gain suppression of the lower SoS stimulus frequency component irrespective of the absolute frequency. Conversely, SVOR and VOR results showed gain enhancement of the lower frequency component and overall decrease in lead. Visually enhanced VOR results showed trends for overall gain suppression and delay decrease.

CONCLUSIONS. Compensatory eye movements arguably depend on predictive signals. These results may reflect better prediction for SS stimuli. Natural CEM system stimulation generally involves complex frequency spectra. Use of SoS stimuli is a step toward unravelling the signals that really drive CEM and the predictive algorithms they depend on.

Keywords: linear systems, eye movement, vestibular system, optokinetic system

Most mammals have an adequate visual system and can respond to visual stimuli through (reflexive) movements of the eyes. The compensatory eye movement (CEM) system attempts to maintain a stable image of the visual field on the retina during head movements. It therefore integrates information from different sensory modalities to enable eye movements that compensate for movements of the visual field.¹ The CEM system is an example of active sensing: used in the motor system in the service of acquiring higher-quality visual information.^{2,3} It comprises two primary reflexes: the vestibulo-ocular reflex (VOR) and the optokinetic reflex (OKR). Although the VOR is often modeled as a linear system,^{4,5} it is known that the OKR is nonlinear. The output of the OKR is predominantly velocity dependent.^{6,7}

Superposition, a key principle of linear systems, states that the response to two inputs combined is the sum of the two input responses in isolation. This property allows us to generalize the system's behavior in conditions that were not explicitly measured. With any combination of stimuli applied, the output eye movements responding to multiple-frequency and amplitude input should satisfy the superposition principle of linear systems (Oppenheim and Schaffer, 1989).⁸ For example, the gain and phase response to a 1.0 Hz single sine

(SS) stimulus presented to the VOR or OKR system should not change; that is, it should have the same gain and phase in a combination 0.8/1.0 Hz sum of sine (SoS; see below) stimulus, or in response to the 1.0 Hz component of a 1.0/1.9 Hz stimulus.

Most oculomotor experimental paradigms explore CEM functional properties using SS waves in a limited range of frequencies and amplitudes.^{6,9–14} Although this approach is ideal for investigating linear systems, it cannot help us understand most nonlinearities, which are known to be present in the oculomotor system.^{6,7} This is especially important because in real-life situations, the CEM system is confronted with multiple inputs that can differ greatly from SS. Single sine stimulation also drives the predictive component of the CEM, controlled by the flocculus of the vestibulocerebellum.^{15–18} Combination of prediction and sensing is a possible source for nonlinearities, analogous to what has been found in smooth pursuit,⁷ and it is important to explore how the system responds under conditions of differing predictability. Although nonsinusoidal stimuli have been used previously in the investigation of the VOR,^{19,20} these have tended to be in the form of broad-band head impulses. Contrastingly, here we used



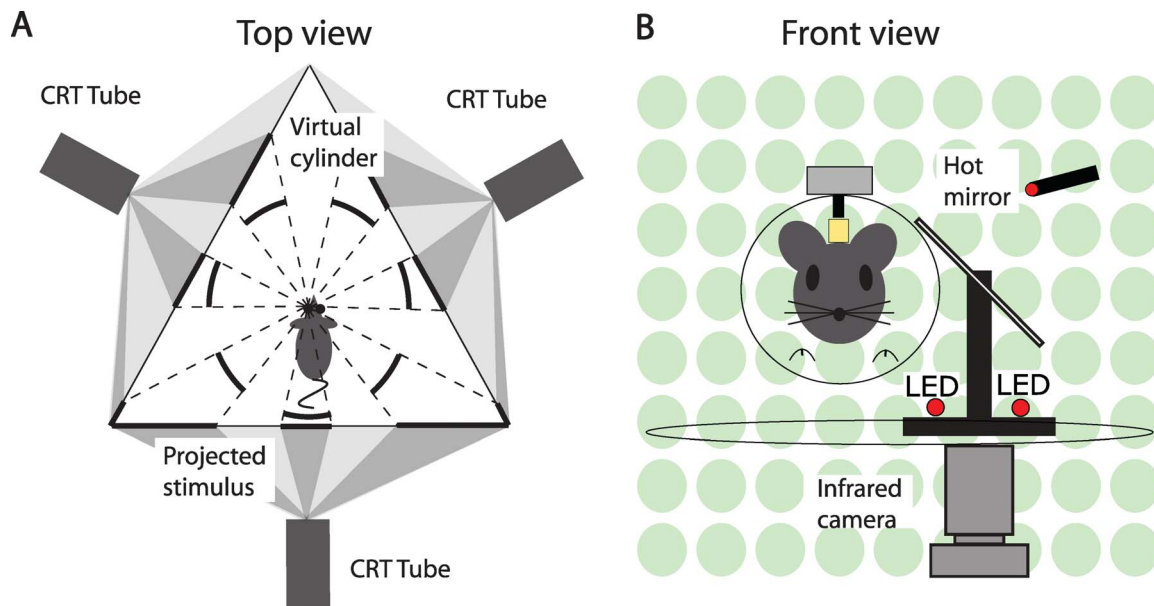


FIGURE 1. (A) Top-down view of mouse in virtual reality setup. Three cathode ray tubes at 120° to each other, projected the virtual panoramic stimuli to the left eye of the mouse in the center of the rotating table. (B) Frontal view of mouse in setup with three infrared LEDs pointing to left mouse eye and image of eye projected to camera under rotating table via the hot mirror.

the less predictable SoS stimuli to investigate long-running nonlinearities.

The constituents of multiple-frequency stimuli can, in nonlinear systems, sometimes generate distortion products in the output, such as occurs with output saturation. Use of noise stimuli has therefore shown to not be ideal, as distortion products will overlap with stimulus frequencies,¹⁷ making analysis difficult. Our aim was to use less predictable SoS stimuli, a combination of multiple sine waves, to tease out the CEM system's ability to satisfy superposition. These frequencies were chosen to be nonharmonic, so as to prevent overlap in the response with putative distortion product frequencies.

MATERIALS AND METHODS

Animal Preparation

Eight adult male mice of the C57BL/6 strain (Charles River, Wilmington, MA, USA) were used in this study. Mice were housed on a 12 hour light/12 hour dark cycle and had unrestricted access to food and water. The experiments were conducted during their light phase. All surgical procedures and experimental protocols were in accordance with the guidelines set by the Animal Welfare Committee of the Erasmus University and the European Communities Council Directive (86/609/EEC) and the ARVO Statement for the Use of Animals in Ophthalmic and Vision Research.

Surgery

We restricted the animals' head movements with a head restraint, which was a prefabricated magnetic pedestal attached to the skull and was made of a light-curing microglass composite (Charisma; Heraeus Kulzer GmbH, Hanau, Germany). We performed all surgical procedures while the animal was anesthetized with a mixture of isoflurane (Isofluran 1.5%–2.0%; Rhodia Organique Fine Ltd., Bristol, UK) and oxygen. After anesthesia induction, a sagittal incision was made across the scalp, exposing lambda

and bregma. The periosteum was removed and the skull was etched using a bristle-tipped applicator dipped in an All-in-One primer and adhesive (Optibond Prime; Kerr USA, Orange, CA, USA). The All-in-One primer was light cured for 5 seconds and air dried for 5 seconds until it formed a hard, shiny layer to facilitate a strong bond between skull and composite. A layer of Charisma was spread over the All-in-One primer and light cured for 1 minute. A second, thicker layer of composite was applied and the magnetic headstage was gently pushed onto this second layer of composite. Animals were allowed to recover for 3 days after surgery and were administered analgesics (0.1 mL buprenorphine [Temgesic]) once daily for 2 days after surgery.

Experimental Setup

The animals were placed in the center of a virtual reality setup that displayed panoramic monochrome stimuli (green dots). The optokinetic stimulus setup has been previously described in detail.²¹ Briefly, the animal was head-fixed and in a mouse restraint designed and built in-house and attached to the table in the recording setup. Dots were projected onto three screens that fully surrounded the animal for a panoramic field of view, thus creating a virtual spherical immersion environment for the mouse (Fig. 1A). The dots were rotated about the vertical axis to stimulate horizontal eye movements. Eye movements were recorded with an infrared video system (ETL-200 with marker tracking modifications; Iscan, Burlington, MA, USA). Images of the eye were captured at 120 Hz with an infrared-sensitive charge-coupled device camera (Iscan). From this image, X and Y positions of the center of the pupil and the corneal reflection were converted to an analog signal and passed to the amplifier for recording. These positions were low-pass filtered and had a cutoff frequency of 300 Hz (Cyberamp 380; Axon Instruments, Union City, CA, USA), sampled at 1 kHz and stored for offline analysis. To keep the field of view as free from obstacles as possible, the camera and lens were mounted under the table surface and recordings were made with a hot mirror that was transparent to visible light and reflective to infrared light (Fig. 1B). The eye was

illuminated with two infrared light-emitting diodes (LEDs) at the base of the hot mirror. Camera, mirror, and LEDs were mounted on an arm that could rotate about the vertical axis over a range of 26.12 degrees (peak to peak). Vestibular stimulation was given by oscillating the table on which the mouse restraint was attached with a servomotor (Mavilor-DC motor 80; Mavilor Motors S.A., Barcelona, Spain). All rotations were about the yaw axis. The driving signal of both the visual and vestibular stimulation, which specified the required position, was computed and delivered by the CED Power1401 data acquisition interface (Cambridge Electronic Design, Cambridge, UK).²¹

Testing Procedure

Stimulus conditions comprised the following four conditions: the OKR, where the visual stimulus was rotated about the head-fixed animal; the VOR, where the animal was rotated on a table in the dark; the visually enhanced VOR (VVOR), where the visual stimulus remained stationary while the animal was rotated; and the suppression VOR (SVOR), where the visual stimulus and the table are rotated in phase, essentially suppressing the functioning of the vestibular system.

Sum of Sine and SS Stimuli

Stimuli used were either single sine (SS) or sum of sine (SoS). In the SoS conditions, frequencies were chosen so as to not be harmonics of each other. Four SS frequencies and four SoS frequency combinations were used in this study. Frequencies presented to the animals for the SS stimuli were 0.6 Hz, 0.8 Hz, 1.0 Hz, and 1.9 Hz. Sum of sine combinations used were 0.6/0.8 Hz, 0.6/1.0 Hz, 0.8/1.0 Hz, and 1.0/1.9 Hz. Amplitude was either 1 or 2 degrees for each frequency (component). For SoS frequencies, either both frequencies had the same amplitude (both 1 degree or both 2 degrees, referred to as 1/1 and 2/2, respectively) or they had different amplitude (one at 1 degree and the other at 2 degrees, referred to as 1/2 when the low frequency component is presented at 1 degree amplitude). This led to a total of 24 types of stimuli in each of the OKR, VOR, VVOR, and SVOR conditions. Thus, we tested each animal with a total of 96 different stimuli in the four conditions. We chose to use relatively small amplitudes in order to avoid nonlinearities that were simply due to saturation of the system because of excessive stimulus velocities.

Stimuli were presented in a fixed sequence for all animals cycling between each of the four stimulus conditions in groups of six. Initially, 6 stimuli were from OKR, then 6 from VOR, 6 from VVOR, 6 from SVOR, then 6 again from OKR, and so on until all 96 stimuli had been presented. Testing took an average of 2 hours for each animal. Stimulus duration ranged from 5.3 seconds (SS, 1.9 Hz stimulus) to 50 seconds (SoS, 1.0/1.9 Hz stimulus), where each stimulus lasted for 10 cycles each.

Data Analysis

Measured eye responses were analyzed offline (Matlab; The MathWorks, Natick, MA, USA). Position signals were transformed into velocity signals by a Savitski-Golay differentiating filter (cutoff frequency 50 Hz with a third degree polynomial) and were then smoothed with a median Gaussian filter (width 50 ms). Nystagmus fast phases and saccades were removed with a velocity threshold of 150 degrees per second and a 10 Hz FIR Butterworth low-pass filter of 50 ms width was then applied. To prevent contamination of the data from any

transient responses to the stimuli, the initial and final 5 seconds of data were removed before analysis of the gain and delay.

There were two primary outcome measures in this study: relative gain and delay (both described subsequently). All statistical analysis was performed on stimuli in which all SS stimuli were presented at amplitude of 2 degrees and SoS with both components presented at 2 degrees amplitude. Statistical analyses were performed by means of repeated measurement ANOVAs separately for relative gains and delays. The ANOVAs compared the relative gain or relative delay of one frequency when it was presented in an SoS combination with other frequencies. If significance was achieved in the ANOVA, two different types of post hoc *t*-tests were performed. The first was paired *t*-tests comparing relative gain or relative delay for the probe frequency across different SoS combinations. The second was 1-sample *t*-tests to test for a difference from a relative gain of 1 or a relative delay of 0 for the probe frequency in each frequency combination. In cases in which the assumption of sphericity was violated (Mauchly's sphericity test, $\alpha = 0.05$), the Greenhouse-Geiser correction was applied and adjusted degrees of freedom are reported in the text. Correction for multiple comparisons in post hoc tests were made by correcting the required significance level using a Sidak correction, in the text the uncorrected *P* value and the corrected α are both reported. For example, in the case of statistical testing of the 1.0 Hz probe frequency, a three-level repeated measures ANOVA (RMANOVA) was performed separately for relative gain and relative delay for each of the four conditions tested. When comparing the delay in the SoS to the delay in the SS components, a separate three-level RMANOVA was performed for each frequency combination in each of the four conditions. In the comparison of relative gains and delays across all pairs tested, a separate eight-level RMANOVA was performed for relative gain and relative delay in the four conditions. Statistical analyses were performed using IBM SPSS Statistics software (Version 21; IBM Corp., Armonk, NY, USA) When presented in the text values are displayed as mean \pm SD.

Power Spectra and Distortion Products

Multifrequency, as well as single-frequency stimulation may introduce distortion products. We generated power spectra using a periodogram method with a hamming window and a nonequispaced fast Fourier transform of 2¹⁵ to show the power of the eye movement responses to check for these distortion products. Given the fact that the OKR is known to saturate at high velocities,⁶ we quantified the amount of distortion present in the power spectra of the eye movement for this condition. Distortion was quantified as the ratio of power in a band with a width of 0.1 Hz centered on each of the stimulus frequencies to the total power below 8 Hz (excluding the stimulus frequencies). Therefore, with increasing distortion, a lower value of this measure will be expected. We then compared the distortion in the SS and SoS conditions across frequencies.

Gain and Delay Calculation

Amplitude and phase information were obtained by fitting sine waves to the stimuli and the data in custom-made Matlab curve-fitting routines using the least-squares method. We used one sine for SS curve fitting and two sines for SoS curve fitting. All fits were visually inspected for accuracy and for the lack of large or non-noise residuals. From the fits of the sine waves to the eye movement data, we then obtained the gain and delay of the eye movements. The gain was calculated as the ratio of the

amplitude of eye movement compared with the amplitude of the stimulus. A gain of 1 signifies perfect tracking where a gain below 1 signifies that the eye moves less than the stimulus.

$$G_{SS}(f) = \frac{E_{SS}(f)}{S_{SS}(f)},$$

where *SS* is for single sine, *f* is the frequency, *G* is gain, *E* is eye movement amplitude, and *S* is stimulus amplitude.

For SoS gains, we fitted two sine waves of the same frequencies as those contained in the stimulus. The amplitude of the fit sine wave for each frequency was compared to the corresponding frequency's amplitude in the stimulus to obtain a gain for each of the constituent frequencies in that SoS stimulus.

$$G_{SoS}(f) = \frac{E_{SoS}(f)}{S_{SoS}(f)}$$

From the gains of SS and SoS, we obtained a relative gain by comparing the two gains for the SoS with their corresponding single sine gains. This allowed us to verify if there was a change in gain of the eye movement response between single sine and SoS stimuli. Thus:

$$G_R(f) = \frac{G_{SoS}(f)}{G_{SS}(f)}.$$

Here, G_R is the relative gain.

A linear system produces, per definition, only relative gains of 1.

Delays (*D*) of single frequencies (or components) were straightforwardly calculated from the phase φ (in radians):

$$D_{SS}(f) = \frac{\varphi_{SS}(f)}{2\pi f}$$

$$D_{SoS}(f) = \frac{\varphi_{SoS}(f)}{2\pi f}.$$

Relative delays (D_R) were calculated by subtracting the SS delay from the SoS delay. Our convention is that a positive delay indicates the eye movement lags behind the stimulus. A positive D_R was indicative of a larger delay or smaller lead in the SoS compared with the SS and a negative D_R indicated a larger delay or smaller lead in the SS.

$$D_R(f) = D_{SoS}(f) - D_{SS}(f)$$

The total delay in the eye movement response to SoS stimuli was calculated by finding the time at which the cross-correlation function of stimulus and eye movement was maximal.

A linear system shows, per definition, only relative delays of 0.

Stability of Response

As SoS stimuli were of longer duration than those with a single component, a separate analysis was performed to check for changes in the gain and delay over time. Sum of sine stimuli were broken into 5 second blocks and the gain and delay of each frequency component was calculated for each block. For each stimulus, a linear regression was performed to calculate the gradient of change of gain or delay across blocks within a stimulus. Subsequently, an RMANOVA was performed separately for each condition (VOR, OKR, VVOR, and SVOR) for both gain and delay, if significance was achieved post hoc 1-

sample *t*-tests were performed to check for differences from a slope of 0.

Asymmetry

To investigate the effect of the amplitude of the individual components in a SoS stimulus on the relative gain and delay, we compared the value for the low-frequency component and the high-frequency component of the stimulus. In the case of relative gains, we took the mean of all of the relative gains of the low-frequency component of the four frequency combinations in a given condition and amplitude combination compared with the mean of the relative gains of the high-frequency component across the same four frequency combinations. If the mean relative gain for both the high- and low-frequency components is the same, then the value will lie on the line of identity when plotted in a scatter plot, values above the line indicate a higher relative gain in the higher frequency component of all pairs. We repeated this procedure for each amplitude combination and condition separately and replicated the entire procedure for the comparison of relative delays.

RESULTS

Compensatory Eye Movement Responses to SS Stimuli

We determined the CEM responses to SS stimuli to establish a baseline for comparison with SoS stimuli. Figure 2 demonstrates that our results are in accordance with oculomotor literature.^{6,7,22} Figures 2A2 and 2A3, respectively, show the gradual increase in VOR gain with increasing frequency and the corresponding decrease in phase lead. Figures 2B2 and 2B3 show the opposite effect for OKR, a decrease in gain with increasing frequency and the associated increase in phase lag. Take note that in Figure 2B3, a high frequency of 1.9 Hz was used, which is well out of the range of the responsiveness of the OKR system.⁶ Figure 2C2 exhibits a near unitary gain at 1 across all frequencies in the VVOR condition and 2C3 shows the associated phase changes. In the SVOR condition in Figures 2D2 and 2D3, we see low gains as expected at lower frequencies due to suppression of the VOR system.

Sum of Sines

A linear system predicts that the summation of two sinusoids is linear; that is, the response to an SoS stimulus is identical to the sum of the responses to its constituent frequencies. In each of the panels in Figure 3, we present, as examples, three traces in each of the four CEM conditions tested with SS stimuli presented with an amplitude of 2 degrees and both components of the SoS stimuli presented at 2 degrees. Each features the 1.0 Hz stimulus (first panel), the 1.9 Hz stimulus (second panel), and the resultant 1.0/1.9 Hz stimulus (third panel) that made up one of the SoS stimuli used in this study. For VOR and OKR, we see a slight lead and a lag, respectively, in the SS 1.0 Hz and 1.9 Hz traces. The VVOR shows good responses to 1.0 Hz and 1.9 Hz, whereas the SVOR shows suppressed responses in the SS traces. For the SoS trace (third panel in each of Figs. 3A-D), we see the SoS physiological response superimposed with the linear prediction; that is, the sum of the two responses to single sines.

Power Spectra

Figures 4A through 4D display the normalized power spectra for stimulus (blue) and eye movement (red) for the SoS

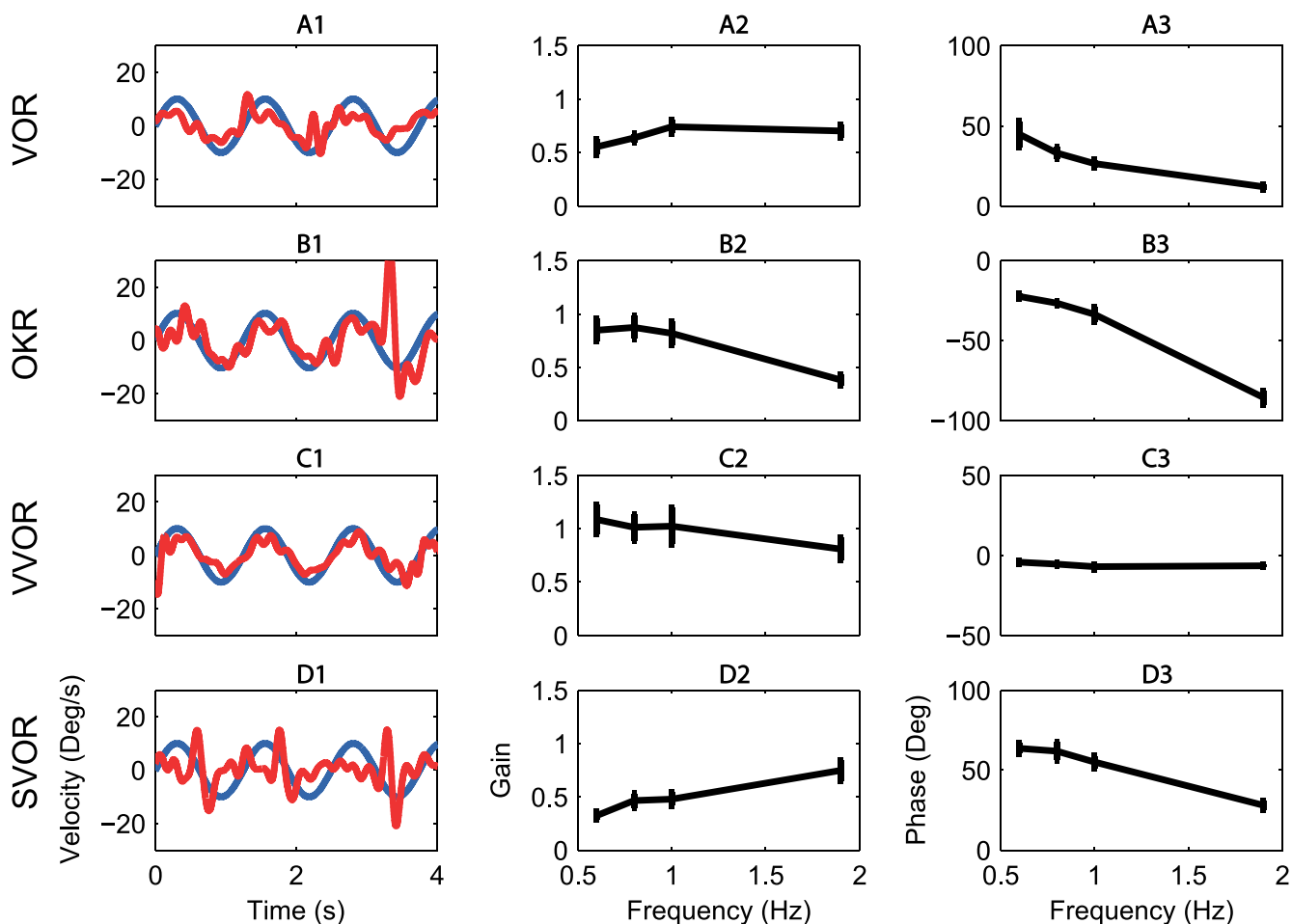


FIGURE 2. Examples of (blue lines) stimulus and eye movement response (red lines) at 1.0 Hz (1), bode plot gains (2), and bode plot phases (3) as functions of SS frequency stimuli in VOR (A), OKR (B), VVOR (C), and SVOR (D). Error bars represent SEM.

combination of 1.0 and 1.9 Hz both presented at an amplitude of 2 degrees for VOR, OKR, VVOR, and SVOR, respectively. Although this example shows clear changes in the power of the constituting frequencies, no consistent or large distortion products are seen, which would show up at frequencies in the eye movement response that are not part of the stimulus spectrum. This was true for all our SoS stimuli. Hence, our remaining analysis was directed at the frequency components that constituted the stimulus.

Following performance of an RMANOVA, there was no effect of frequency pair on the level of distortion in the OKR for either SoS stimuli ($F_{3,7} = 0.34$, $P = 0.796$, partial $\eta^2 = 0.05$) or SS stimuli ($F_{3,7} = 1.54$, $P = 0.235$, partial $\eta^2 = 0.18$). Single-sine stimuli had lower values (0.33 ± 0.21 for SS, 0.54 ± 0.16 for SoS) of this measure, indicating a lower ratio of power at stimulus frequency to other frequencies. However, this can be explained by the fact that the SoS stimuli had two frequency bins and therefore a greater degree of power within this in comparison to the rest of the power below 8 Hz.

Stability of Response

For the longer duration SoS stimuli, it is important to know that any differences in relative gain or delay are not due to changes in the nature of the response over time that may possibly be due to factors such as fatigue, habituation, or dryness of the mouse eye. Additionally, time may indeed be a factor in making predictions about the stimuli. To check for such changes, the

gain and delay of the response was analyzed in 5 second blocks and linear regression performed to give the gradient of the slope of any change. We found no effect of component frequency on the gradient for any condition in terms of either gain (VOR $F_{1,69,7} = 1.04$, $P = 0.372$, partial $\eta^2 = 0.13$; OKR $F_{7,7} = 0.67$, $P = 0.693$, partial $\eta^2 = 0.09$; VVOR $F_{7,7} = 0.31$, $P = 0.947$, partial $\eta^2 = 0.04$; SVOR $F_{2,113,7} = 0.55$, $P = 0.791$, partial $\eta^2 = 0.07$) or delay (VOR $F_{1,92,7} = 0.87$, $P = 0.570$, partial $\eta^2 = 0.11$; OKR $F_{7,7} = 0.71$, $P = 0.666$, partial $\eta^2 = 0.09$; VVOR $F_{1,97,7} = 1.63$, $P = 0.150$, partial $\eta^2 = 0.19$; SVOR $F_{3,06,7} = 1.63$, $P = 0.212$, partial $\eta^2 = 0.19$).

Sum of Sines Analyses

In our analyses, we show SoS results for a probe frequency stimulus, 1.0 Hz in combination with flanker frequencies of 0.6 Hz, 0.8 Hz, and 1.9 Hz. Thus, the probe frequency is sometimes the higher frequency and sometimes the lower frequency of the SoS pair. Subsequently, we show that these results can be extrapolated toward our other frequency combinations as well.

Relative Gains of the 1.0 Hz Component

Overall, we see that the relative gains in response to SoS stimuli are not all at unity gain of 1, indicating the presence of nonlinearities. In the VOR paradigm, the relative gain (Fig. 5A1) was significantly different among the three frequency combi-

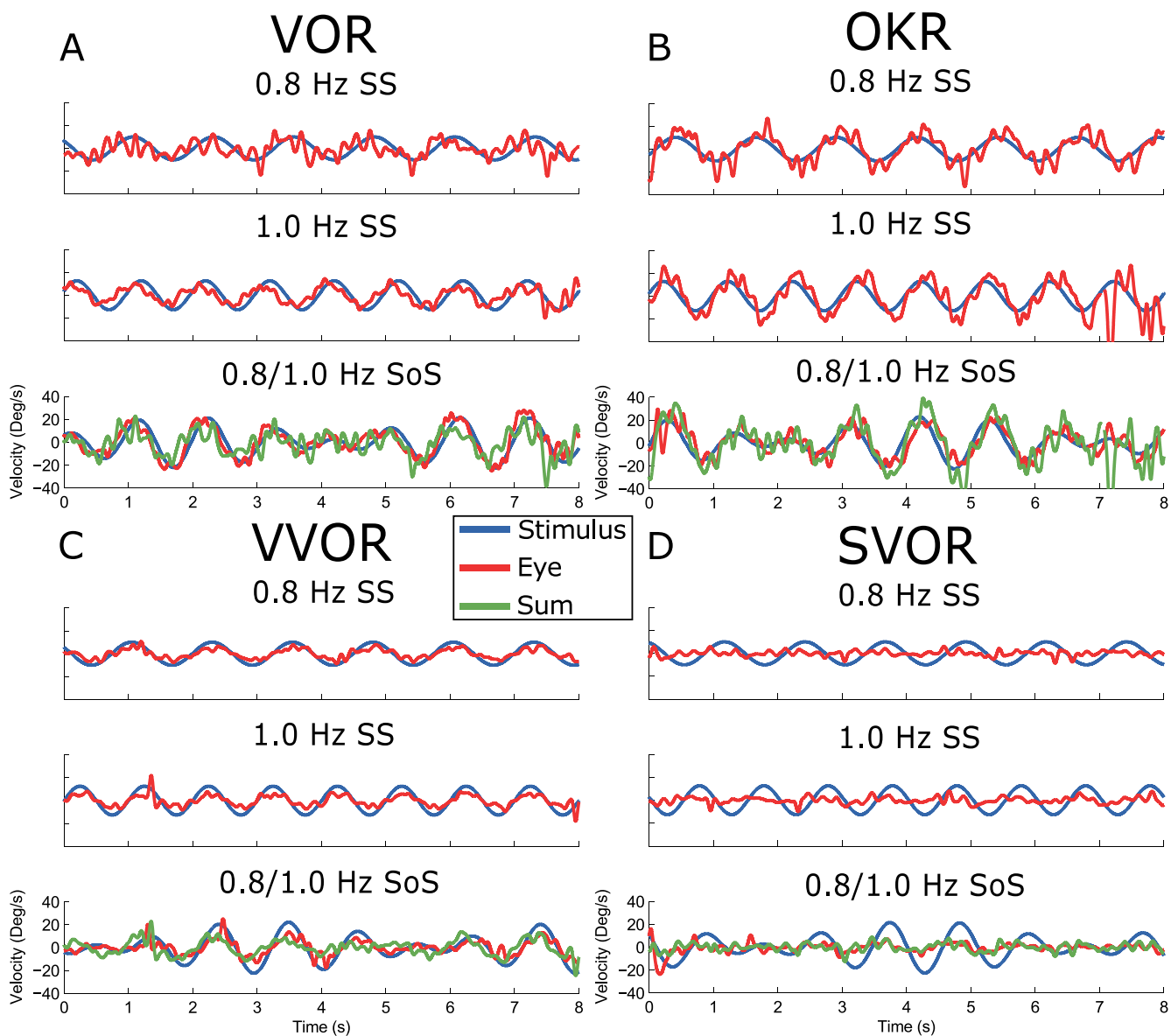


FIGURE 3. Examples showing combination of 0.8 Hz SS (top), and 1.0-Hz SS (middle) to give the SoS 0.8/1.0 Hz stimulus (bottom) and associated eye movement in VOR (A), OKR (B), VVOR (C), and SVOR (D). Blue: stimulus; red: eye movement response; green: linear summation of the two SS responses.

nations ($F_{2,7} = 6.99$, $P = 0.008$, partial $\eta^2 = 0.50$). Post hoc comparisons revealed that the relative gain of the 1.0 Hz component was higher when presented in combination with the 1.9 Hz stimulus than in the 0.6/1.0 Hz SoS ($P = 0.015$) and the 0.8/1.0 Hz SoS ($P = 0.035$); however, only the difference between the 1.0/1.9 Hz and 0.6/1.0 Hz remained significant after correction for multiple comparisons ($\alpha = 0.017$). Additionally, none of the relative gains were significantly different than 1. In the OKR paradigm (Fig. 5B1), the combination did affect the relative gain ($F_{1,12,7} = 23.34$, $P = 0.001$, partial $\eta^2 = 0.77$). Post hoc pairwise comparisons showed that the gain of the 1.0 Hz was lower in the 1.0/1.9 Hz combination than in the other two combinations (both $P < 0.005$). Moreover, only in the 1.0/1.9 Hz condition was the relative gain significantly smaller than 1 (i.e., a lower gain in the SoS than in the associated SS) (0.24 ± 0.09 , $t[7] = -23.47$, $P < 0.001$). In the VVOR paradigm (Fig. 5C1), the relative gain was not different between frequency combinations ($F_{2,7} =$

0.05 , $P = 0.950$, partial $\eta^2 = 0.01$) and none were significantly different than 1. Finally, in the SVOR paradigm, the frequency combination did have an effect on the relative gain ($F_{2,7} = 72.14$, $P < 0.001$, partial $\eta^2 = 0.91$). Post hoc pairwise comparisons showed the relative gain to be higher in the 1.0/1.9 Hz combination than in the other two combinations (both $P < 0.001$). Additionally, only in the 1.0/1.9 Hz combination was the relative gain significantly greater than 1 (1.77 ± 0.35 , $t[7] = 6.28$, $P < 0.001$).

From these results, we see an opposing effect on the 1.0 Hz component in the OKR compared with the SVOR condition (Figs. 5B1, 5D1). In OKR, 1.0 Hz is suppressed (Fig. 5B1) when it is the lower frequency (combined with 1.9 Hz). Its gain remains unchanged when it is the higher frequency component; that is, when combined with 0.6 Hz and 0.8 Hz. In contrast, in the SVOR paradigm (Fig. 5D1) the gain is enhanced when presented as the lower frequency component in a SoS stimulus but remains unchanged when presented in combina-

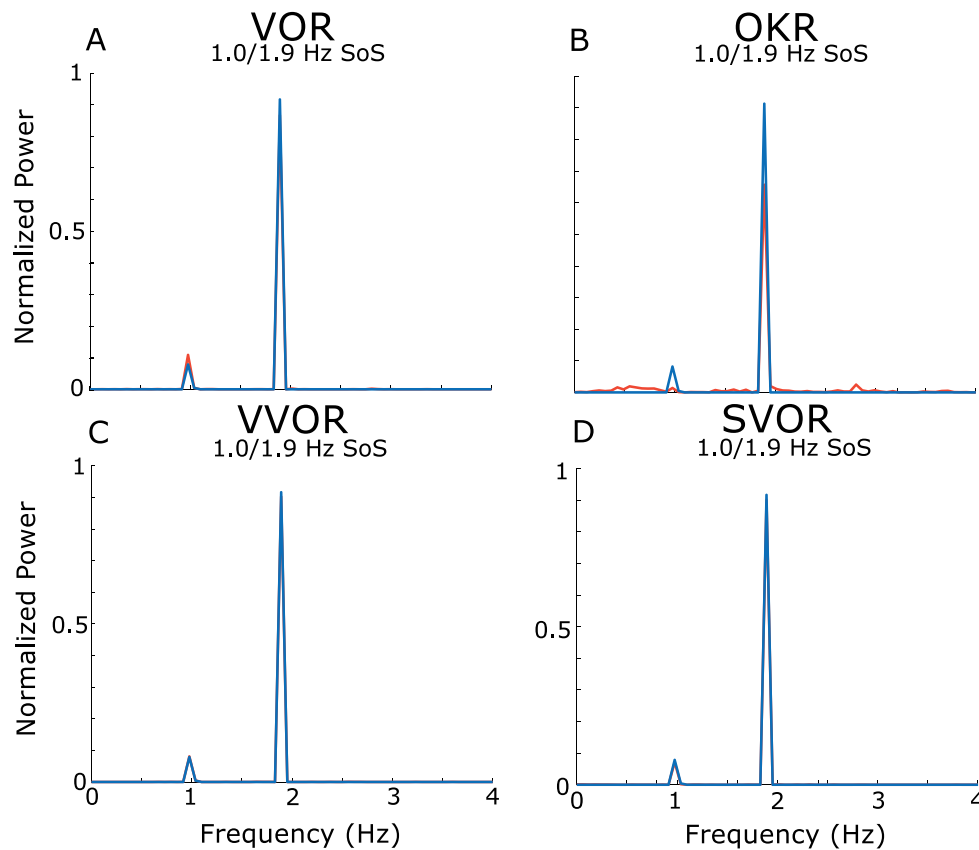


FIGURE 4. Power spectra of stimulus (blue) and movement (red) for SoS of 1.0 and 1.9 Hz for (A) VOR, (B) OKR, (C) VVOR, (D) SVOR. These examples show no introduction of distortion products.

tion with a lower frequency. We also see an effect on relative gain in VOR but at the same time none of the relative gains were calculated to be significantly different from 1.

Relative Delays of the 1.0 Hz Component

Overall, we show the presence of nonlinearities in terms of relative delays (Figs. 5A2, 5B2, 5C2, 5D2) in the responses to SoS stimuli, as not all relative delays were 0. In the VOR paradigm, the combination did significantly affect the relative delay ($F_{2,7} = 7.91$, $P = 0.005$, $\eta^2 = 0.53$), post hoc comparisons revealed the relative delay of the 1.0 Hz component in the 1.0/1.9 Hz combination was significantly greater than in both the 0.6/1.0 Hz SoS ($P = 0.013$) and the 0.8/1.0 Hz SoS ($P = 0.039$); however, only the difference between the 1.0/1.9 Hz and 0.6/1.0 Hz remaining significant after correction for multiple comparisons ($\alpha = 0.017$). Furthermore, the relative delay of the 1.0 Hz component in both the 0.8/1.0 Hz and the 1.0/1.9 Hz combinations was significantly greater than 0, indicating a decreased lead of movement over stimulus (0.027 ± 0.020 seconds, $t[7] = 3.75$, $P = 0.001$ and 0.044 ± 0.022 SD, $t[7] = 5.59$, $P = 0.001$, respectively). In the OKR paradigm, the frequency combination significantly affected the relative delay ($F_{1,04,7} = 24.10$, $P = 0.001$, partial $\eta^2 = 0.78$). The delay for the 1.0 Hz probe frequency was greater in the 1.0/1.9 Hz combination than in both the 0.8/1.0 Hz combination ($P = 0.001$) and the 0.6/1.0 Hz combination ($P = 0.003$), indicated by a positive relative delay. Furthermore, the 1.0 Hz relative delay in the 1.0/1.9 Hz (0.11 ± 0.06 seconds, $t[7] = 4.91$, $P = 0.002$) frequency combination was significantly greater than a relative delay of 0, indicating an increased delay when

presented as the lower frequency of a pair. In the VVOR paradigm, no effect of frequency combination on relative delay was observed ($F_{2,7} = 1.18$, $P = 0.336$, partial $\eta^2 = 0.14$). In the SVOR paradigm, relative delay was affected by frequency combination ($F_{2,7} = 101.28$, $P < 0.001$, partial $\eta^2 = 0.94$). The delay for the 1.0 Hz probe frequency was greater in the 1.0/1.9 Hz combination than in the other two combinations (both $P < 0.001$). Moreover, only the relative delay in the 1.0/1.9 Hz frequency combination was significantly greater than 0 (0.099 ± 0.026 seconds, $t[7] = 10.72$, $P < 0.001$).

From the delay information in all of the paradigms, we did not see any response leads (in the case of VOR and SVOR) becoming delayed responses or vice versa. In all cases, the delays present in SS responses never decreased when used in SoS or the lead (in the case of VOR and SVOR) never grew larger. The exception to this is the trend for smaller delays (negative relative delays) in VVOR; however, this failed to reach significance for any component.

Generalization to Other Frequency Combinations

The results using 1.0 Hz as a probe frequency show that the relative gain and phases of the probe frequency depends on the other frequency that it is combined with. It seems to be suppressed when it is the lower frequency in OKR and enhanced when it is the lower frequency in SVOR. We observed the same result when we used 0.8 Hz as the probe frequency, in combination with a lower frequency (0.6 Hz) or with a higher frequency (1.0 Hz). This is evidence of

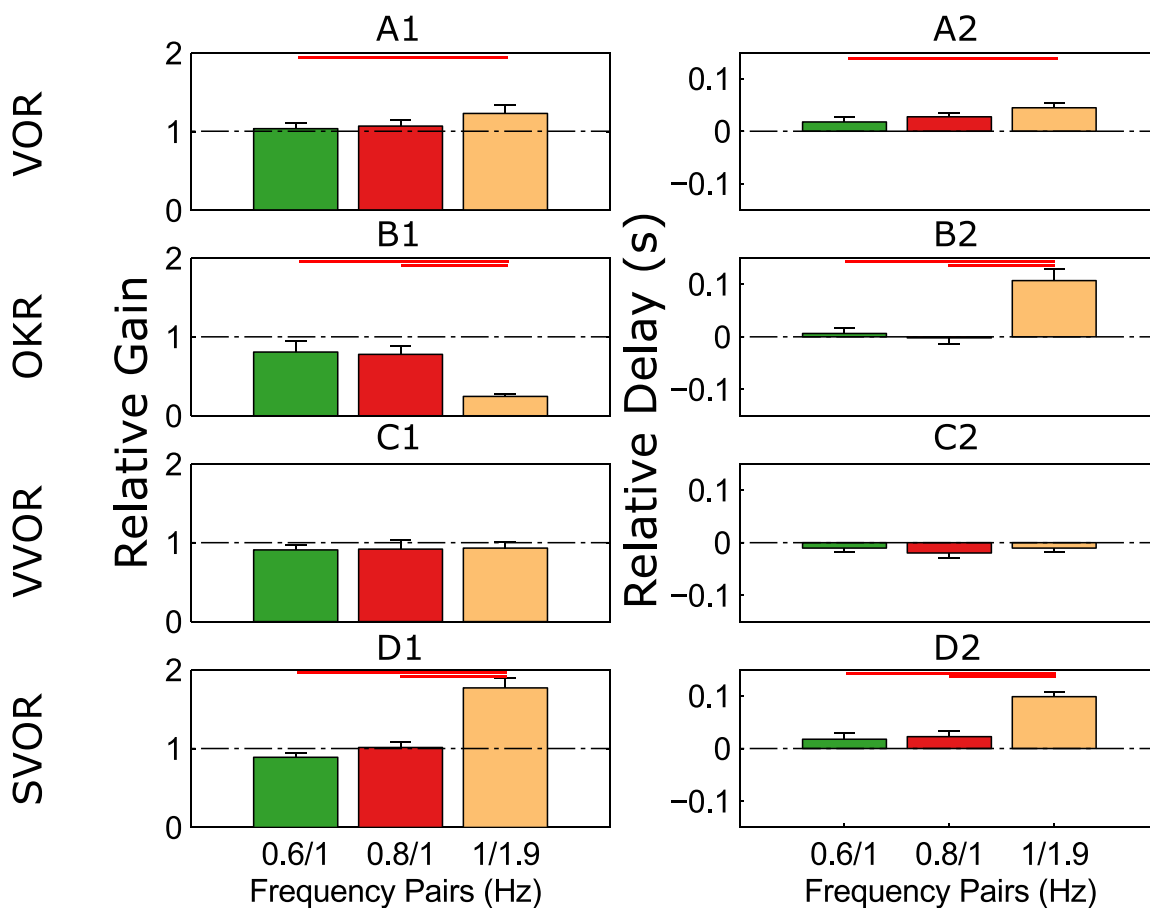


FIGURE 5. Effect on the relative gain and delay of the 1 Hz probe frequency when paired with different flanker frequencies. Nonlinear responses are evidenced by the fact that the mean relative gain and delay differs depending on which frequency the probe was presented alongside. (A–D) The results for VOR, OKR, VVOR, and SVOR, respectively, illustrating the opposing effect in OKR and SVOR. Horizontal red lines above the bars indicate a significant difference between the underlying pair at the $\alpha = 0.05$ level, corrected for multiple comparisons. Error bars represent SEM.

nonlinearity in the CEM system that is not restricted to a specific frequency.

Total Delays in SoS Compared With SS Delays

The more complex SoS signals may trigger a more delayed response than the predictable SS signals. Combination of stimuli may have changed an SS response from a lead to it being a delay when its component in the SoS condition is compared with the SS condition. Total delay analysis showed that no responses that were a delay in the SS condition turned to a lead in the SoS condition or vice versa. These data compared the total delays in the response to an SoS stimuli in comparison with the delay in response to the high- and low-frequency component when presented in isolation (SS) for all four frequency pairs. In the VOR, there is a significant effect of component on delay in all four frequency combinations (0.6/0.8 Hz, $F_{2,7} = 6.53$, $P = 0.01$, partial $\eta^2 = 0.48$; 0.6/1.0 Hz, $F_{1,09,7} = 13.744$, $P = 0.006$, partial $\eta^2 = 0.66$; 0.8/1.0 Hz, $F_{2,7} = 25.09$, $P < 0.001$, partial $\eta^2 = 0.78$; 1.0/1.9 Hz, $F_{1,17,7} = 83.02$, $P < 0.001$, partial $\eta^2 = 0.92$). Post hoc comparisons revealed that the effect was mainly due to a difference in the total SoS delay compared with the lower-frequency SS component, with a smaller lead (indicated by a less negative delay) in the SoS. For all frequency combinations (0.6/0.8 Hz, 0.6/1.0 Hz, 0.8/1.0 Hz, and 1.0/1.9 Hz) there is a significantly smaller lead in the total SoS compared with the lower-frequency SS ($t[7] = 2.705$, $P = 0.03$; $t[7] = 3.797$, $P = 0.007$; $t[7] = 6.259$, $P < 0.001$; $t[7] =$

9.354, $P < 0.001$, respectively). However, the effect in the 0.6/0.8 Hz combination was not significant after correction for multiple comparisons ($\alpha = 0.017$). There is also a smaller lead in response to SoS when compared with the higher-frequency SS for the 0.8/1.0 Hz combination ($t[7] = 3.961$, $P = 0.005$).

In the OKR, the only frequency pair that showed a significant effect of component on delay was the 1.0/1.9 Hz combination ($F_{2,7} = 12.62$, $P = 0.001$, partial $\eta^2 = 0.64$). Pairwise comparisons revealed that here the SS lower-frequency delay is smaller than the total SoS delay ($t[7] = 3.604$, $P = 0.009$).

For the VVOR in only one frequency pair (1.0/1.9 Hz) was there a significant effect of component on delay ($F_{2,7} = 5.69$, $P = 0.016$, partial $\eta^2 = 0.45$). Pairwise comparisons revealed a greater delay in the 1.0 Hz SS in comparison with the total delay in the 1.0/1.9 Hz SoS; however, this failed to reach significance after correction for multiple comparisons ($t[7] = -2.642$, $P = 0.033$, $\alpha = 0.017$). Although there is generally a greater delay in SS than the SoS in the VVOR, this trend failed to reach significance.

Suppressed VOR exhibits similar results to VOR, whereby all frequency combinations contained a significant effect of component on delay (0.6/0.8 Hz, $F_{2,7} = 27.88$, $P < 0.001$, partial $\eta^2 = 0.80$; 0.6/1.0 Hz, $F_{2,7} = 17.30$, $P < 0.001$, partial $\eta^2 = 0.91$; 0.8/1.0 Hz, $F_{2,7} = 15.27$, $P < 0.001$, partial $\eta^2 = 0.69$; 1.0/1.9 Hz, $F_{1,1,7} = 133.84$, $P < 0.001$, partial $\eta^2 = 0.95$). Post hoc pairwise comparisons revealed here is a smaller lead (less-negative delay) in response to SoS stimuli compared with the

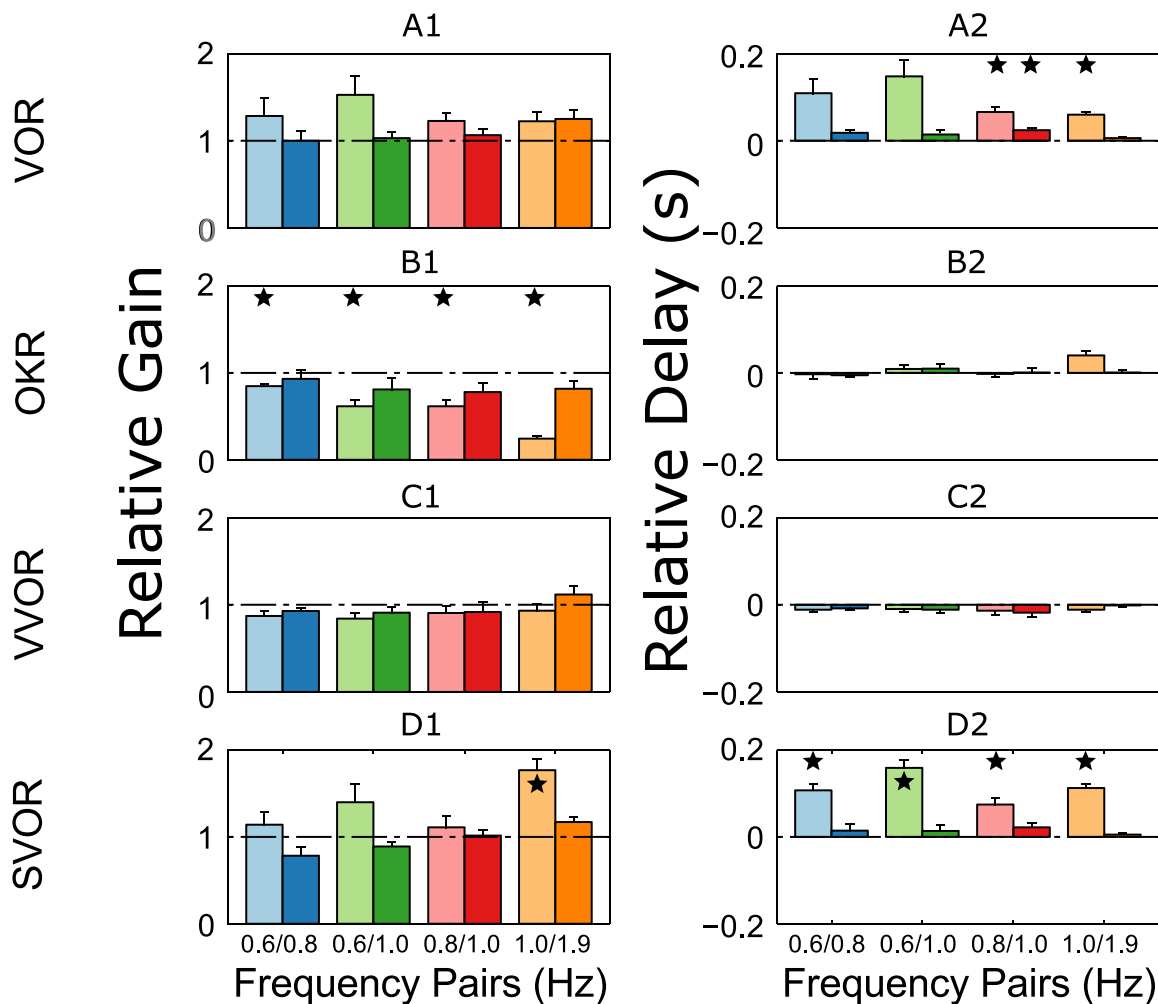


FIGURE 6. Relative gains and delays for all components of the four frequency combinations (all presented at an amplitude of 2 degrees). Rows (A–D) represent VOR, OKR, VVOR, and SVOR, respectively, with the *left column* containing *bar graphs* depicting the mean relative gain and the *right column* the mean relative delay. The presence of consistent differences between components of a frequency pair indicates nonlinear responses. *Error bars* represent SEM and *stars* on or above the *bars* mark significant difference from 1 (relative gains) or 0 (relative delays) at $\alpha = 0.05$ level, corrected for multiple comparisons.

lower frequency SS in all four frequency pairs ($t[7] = 4.097 - 11.469, P = 0.000 - 0.005$).

Figure 6 details the mean relative gains and relative delays in all four CEM conditions tested for all SoS frequency combinations. Assuming linearity of the CEM system, we would expect the relative gains to be at unity (1). Overall, we see that the relative gains are not at unity and we see there is a consistent pattern in the relative gain of each component of a SoS frequency pair in some of the CEM conditions (see below). In the VOR paradigm (Fig. 6A1), there was no significant effect of frequency on relative gain across the eight SoS components ($F_{1,724,7} = 3.074, P = 0.089$, partial $\eta^2 = 0.31$); however, there is a strong trend. For OKR (Fig. 6B1) there was a significant effect of frequency component on relative gain ($F_{7,7} = 8.78, P < 0.001$, partial $\eta^2 = 0.56$). Post hoc comparisons revealed that for all four of the lower-frequency components of the SoS pairs, gains are significantly less than 1 (0.6/0.8 Hz, $0.84 \pm 0.08, t[7] = -5.41, P = 0.001$; 0.6/1.0 Hz, $0.61 \pm 0.21, t[7] = -5.19, P = 0.001$; 0.8/1.0 Hz, $0.61 \pm 0.19, t[7] = -5.79, P = 0.001$; 1.0/1.9 Hz, $0.24 \pm 0.09, t[7] = -23.45, P < 0.001$). In contrast, the higher frequencies of the SoS pair did not significantly differ from unity gain. Visually enhanced VOR relative gains (Fig. 6C1) were not significantly affected by SoS frequency

component ($F_{2,2,7} = 1.72, P = 0.210$, partial $\eta^2 = 0.20$). For SVOR (Fig. 6D1) relative gain was significantly affected by SoS frequency component ($F_{7,7} = 11.65, P < 0.001$, partial $\eta^2 = 0.63$). Post hoc tests revealed only one component differing from unity gain: 1.0 Hz of 1.0/1.9 Hz ($1.77 \pm 0.35, t[7] = 6.266, P < 0.001$). Interestingly, there was a trend for the lower-frequency component of a pair to have a higher relative gain when compared with its partner; post hoc pairwise comparisons revealed this to be significant for both the 0.6/0.8 Hz and 1.0/1.9 Hz combinations ($P = 0.005$ and $P = 0.002$, respectively).

The panels on the right of Figure 6 display mean relative delays for each frequency component in the four SoS pairs tested. In the case of VOR (Fig. 6A2), there was a significant effect of component on the relative delay ($F_{1,279,7} = 10.37, P = 0.008$, partial $\eta^2 = 0.60$). Post hoc test revealed that three components had a relative delay significantly higher than 0: 0.8 Hz of 0.8/1.0 Hz ($0.066 \pm 0.030, t[7] = 6.26, P < 0.001$), 1.0 Hz of 0.8/1.0 Hz ($0.024 \pm 0.017, t[7] = 3.961, P = 0.005$), and 1.0 Hz of 1.0/1.9 Hz ($0.060 \pm 0.018, t[7] = 9.36, P < 0.001$). There was also a visible trend for the lower frequency component of the pair to have a higher relative delay than its partner; pairwise comparisons revealed a significant difference

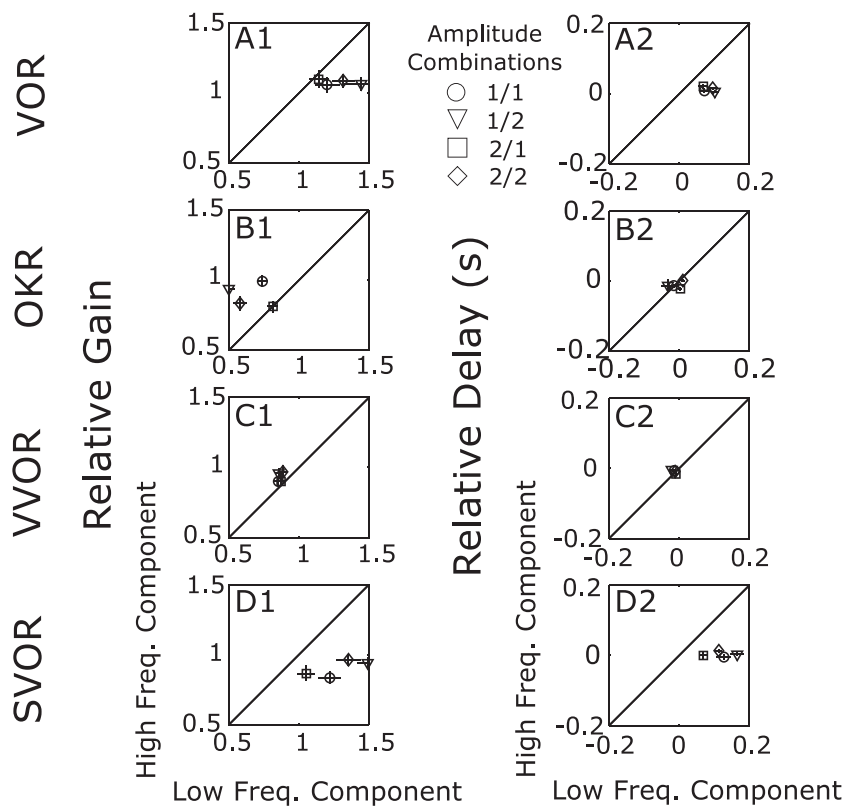


FIGURE 7. Comparison of the mean relative gain (left column) and delay (right column) for different amplitude SoS stimuli. (A–D) Results for VOR, OKR, VVOR, and SVOR, respectively. The x-axis is the mean value for all lower frequency components of the four pairs, whereas the y-axis is the mean value of the high-frequency components. The line of identity is marked and points lying away from this indicate deviations for linear summation. Although changing the amplitude of the individual components affects the magnitude of the effect, in no case does it reverse the directions of the asymmetry between pairs. Horizontal and vertical error bars represent SEM of the low-frequency and high-frequency components, respectively.

in all frequency pairs except 0.6/0.8 Hz (0.6/1.0 Hz, $P = 0.008$; 0.8/1.0 Hz, $P = 0.006$, 1.0/1.9 Hz, $P < 0.001$). In the case of VOR as the usual response is a lead of movement over stimulus, a positive relative delay indicates a smaller lead in the SoS than in the SS for that particular component.

For OKR (Fig. 6B2), there was a significant effect of component on relative delay ($F_{7,7} = 4.25$, $P = 0.001$, partial $\eta^2 = 0.38$). Post hoc pairwise comparisons revealed a significantly higher relative delay in the 1.0 Hz component of the 1.0/1.9 Hz pair than in the 1.9 Hz component ($P = 0.005$). Although this component showed a strong trend for being greater than 0 (0.039 ± 0.031 , $t[7] = 3.60$, $P = 0.009$), this did not meet the corrected level of significance ($\alpha = 0.0064$).

There was no significant effect of component on the relative delay in response to VVOR (Fig. 6C2) stimulation ($F_{7,7} = 0.64$, $P = 0.722$, partial $\eta^2 = 0.08$). In the case of SVOR (Fig. 6D2), component did significantly affect relative delay ($F_{7,7} = 35.66$, $P < 0.001$, partial $\eta^2 = 0.84$). Post hoc testing revealed all four of the lower frequencies of the SVOR SoS pairs to be significantly greater than a relative delay of 0: 0.6 Hz of 0.6/0.8 Hz (0.11 ± 0.04 , $t[7] = 7.41$, $P < 0.001$), 0.6 Hz of 0.6/1.0 Hz (0.16 ± 0.05 , $t[7] = 9.24$, $P < 0.001$), 0.8 Hz of 0.8/1.0 Hz (0.07 ± 0.05 , $t[7] = 4.54$, $P = 0.003$), and 1.0 Hz of 1.0/1.9 Hz (0.11 ± 0.03 , $t[7] = 11.47$, $P < 0.001$); contrastingly, none of the high-frequency components differed from 0. Post hoc pairwise testing also indicated that for all four frequency pairs, the two components were significantly different from each other (all $P < 0.006$).

From these significant differences from unity relative gain and 0 relative delay, we can infer the violation of the

superposition principle of linear systems and the presence of nonlinearities in the CEM system in response to SoS stimulus conditions. We also note that at all frequency combinations in OKR, we see suppression in the relative gains of the lower-frequency stimulus compared with the higher-frequency stimulus. The opposite phenomenon is true for the SVOR condition; that is, the lower frequency of the SoS pair is enhanced whereas the higher frequency component remains unchanged. Another consistent finding is the decrease in lead in VOR and SVOR when a given SS frequency stimuli is presented in combination with another frequency; this effect seems especially pronounced in the lower-frequency component of a pair.

Asymmetry

All of the results presented so far have used solely the data in which the SS stimuli were presented with an amplitude of 2 and both components of an SoS were also at amplitude 2 (referred to as 2/2). Figure 7 shows our asymmetry results, which details all the amplitude conditions used in all the CEM conditions. The mean relative gains for the lower frequency of the SoS pairs are compared against the mean relative gains of the higher frequency of the SoS pairs to display any asymmetries present for all the amplitude conditions. Relative delay results are presented similarly in the second column of Figure 7. From our asymmetry results, we see that all our values obtained for gains and delays remain on the same side of the line of identity, indicating that the general patterns

described above are present in all amplitude conditions tested.

DISCUSSION

Most literature on CEM uses predictable SS stimuli to understand how the oculomotor system works.^{6,9-16,21,23-25} Our dataset goes further by also exploring the CEM system's response to less-predictable SoS stimuli. Our results do reiterate nonlinearity and question the importance of using SS stimuli on a system that is well known to be nonlinear.^{6,7} We suggest that more complex and less-predictable (SoS) stimuli should be used to fully investigate the functioning of the oculomotor system to more realistic stimuli. Our data find the presence of nonlinearities in the OKR, VOR, and SVOR conditions. We did not find any significant nonlinearities in the VVOR condition. The nonlinearities reported are indicative of a violation of the superposition principle (Oppenheim and Schaffer, 1989),⁸ a hallmark of linear systems (see the first paragraphs of this article). These nonlinearities are observed as changes in amplitude (gain) and/or timing (delay) of responses to less-predictable sinusoidal stimulation (Figs. 5-7), when these stimuli are presented in tandem with other frequencies.^{26,27} Meanwhile, in none of the CEM responses were distortion products observed (Fig. 4), which means that these were either absent or too small to detect in the oculomotor recordings.

The VOR system of mice has been previously indicated to not obey the homogeneity principle of linear systems. Iwashita et al.²⁸ reported that the VOR gain in mice exhibited dependence on the angular acceleration of head turn. When the angular amplitude of head oscillation was set higher at a specific frequency, the gain was seen to increase. Van Alphen et al.²⁹ showed that in mice, the VOR gain decreased proportionally to velocity for faster stimuli. The VOR response changed with stimulus amplitude, giving a higher gain and lower-phase lead with increasing stimulus amplitude. This nonlinear response showed that reflex gain correlated strongly with stimulus acceleration.²⁹

Previous nonlinearities in the VOR system have been reported in the literature for species other than mice. Dow et al.³⁰ and Sudlow et al.³¹ showed that the VOR in habituated goldfish violated the homogeneity principles of linear systems. These data suggested that the VOR is indeed nonlinear and questioned the practice of modeling the VOR as a linear system. They habituated goldfish VOR at a lower frequency (0.01 Hz) and then combined it with a higher frequency (0.3 Hz). Their results showed a 10-fold increase in the gain of the habituating frequency indicative of a severe violation of the superposition principle.³⁰ Massot et al.²⁰ showed in monkeys that vestibular sensory information encoded by the VIIIth nerve afferents is integrated nonlinearly by postsynaptic central vestibular neurons. They categorized this nonlinear response by a strong (50%) reduction in neuronal sensitivity to low-frequency stimuli when presented simultaneously with high-frequency stimuli. Their results challenged the conventional perception that the vestibular system uses a linear rate code to transmit information. Minor et al.³² tested the horizontal VOR in squirrel monkeys via high-acceleration rotations. Monkeys with an intact vestibular system showed reflex gains during the acceleration to be $14.2\% \pm 5.2\%$ greater than that measured once the plateau head velocity had been reached. Animals that had undergone bilateral labyrinthectomy had negligible responses to the acceleration stimuli. Inputs to the VOR reflex came from linear and nonlinear pathways. The frequency and velocity dependent nonlinearity in VOR gain is accounted for by the dynamics of the nonlinear pathway.³¹

Single Sines

Our results for responses to predictable SS stimuli are in accordance with the accepted literature on CEM. As expected, the optokinetic system is more sensitive to low velocity stimuli and the vestibular system is more responsive to higher frequency stimuli.^{6,7,19,29} In this way, the two systems are complementary to each other (Figs. 2A2, 2B2). During VVOR, these two systems work in conjunction, yielding near perfect responses (i.e., unity gain and no delay; Figs. 2C2, 2C3). Finally, visual suppression during SVOR is more effective at low velocities, because the optokinetic response is strong in this range, resulting in more effective suppression in these conditions.^{7,33}

Sum of Sines

With SoS stimulation, we were able to show the superposition violations in the optokinetic and vestibular systems (summarized in Figs. 5-7). Both the OKR and SVOR components of the probe frequency of 1.0 Hz show relative gains that deviate significantly from 1. This effect is most strongly observed when the probe frequency is combined with a frequency that is higher (rightmost bars of Figs. 5B, 5D), resulting in a decrease of the OKR response, and an increase of the SVOR. This is in mutual agreement with each other, as the optokinetic signal is the suppressing signal in SVOR. Hence, less OKR will lead to stronger SVOR responses. Utilization of another probe frequency (0.8 Hz) showed similar results to those of the 1.0 Hz probe frequency seen in Figure 5, suggestive of systematic deviation from superposition of a linear system. This superposition deviation is seen across all frequency pairs in Figure 6B1.

Eye movement delay also supports the evidence of superposition violation in the CEM system. The responses to the 1.0 Hz stimulus do not show a relative delay of 0 when combined with other frequencies, in all movement types except the VVOR (Figs. 5, 6). Likewise, comparing total SoS delay with the SS delays, there is a greater delay in the SoS compared with SS; in the case of VOR and SVOR, this indicates a decreased lead and in OKR and VVOR an increased lag. Like for the gains, the strongest effects were observed when the probe frequency was combined with a relatively higher frequency. Again, similar results were found when using the 0.8 Hz stimulus as probe frequency.

Prediction

The CEM system is engaged in active sensing. Active sensing can be defined as motor activity for the purpose of acquiring sensory information, such as moving the eyes to see something.^{2,3} Central to active sensing is the role of prediction signals. Predictions from a forward model can be faster and less noisy than the full sensory loop, although predictions of the state must be combined with actual sensory feedback for the control loop to remain robust in the face of unpredicted perturbations.³⁴

In our data, responses to SS in CEM more closely track the stimulus than during SoS stimulation. Gains are closer to 1 and delays are smaller or leads are larger. When using traditional SS stimuli, there is a certain predictability in the stimulus.³⁵ We therefore hypothesize the presence of a prediction signal in SS stimuli that is not present in the SoS stimuli. This prediction signal is akin to what is observed in smooth pursuit, where the more complex and unpredictable a stimulus becomes, the more impaired the pursuit reflex becomes.⁷

For CEM prediction, a forward model in the flocculus of the vestibulocerebellum may provide a provisional state estimation used to stabilize feedback control.³⁴ The flocculus of the vestibulocerebellum is known to play a role in the control of

eye movements.^{11,15–18,36,37} We hypothesize that SoS stimuli are much harder to anticipate and this reduces the contribution of the flocculus during SoS stimulation.

The presence of a prediction signal would allow an animal that tracks an SS stimulus to achieve a more veridical response, because it does not have to react to sensory stimulation only. Actual retinal slip that results from self-motion may actually be sine-like, or at least have a clear dominant frequency, as locomotion is repetitive and regular. However, to our knowledge, no data exist on this in mice or other rodents.

Further experimentation to illustrate the predictive capability of the CEM system in response to SoS stimulation could come from computational modeling techniques. Testing the presence or absence of a prediction signal in SS and SoS stimuli via the state predicting feedback control model of Frens and Donchin³⁴ would lend support to our data set here showing superposition violations.

Relative Frequencies

Strikingly, all superposition violations that we observed were most prominent when the probe frequency was combined with a higher frequency, despite the highly different dynamical properties of the different CEM systems per se (Fig. 2, SS bode plots). Thus, it seems as if a larger importance is assigned to the higher frequency. One might speculate that this is because higher frequencies may result in higher slip velocities, and hence blur vision more strongly.

Saturation

It could be said that the nonlinearities we report are due to high velocities and amplitudes and, thus, a velocity saturation effect of the VOR and OKR systems.^{31,38} At high velocities and high amplitudes, there is saturation of the velocity-sensitive neurons on the retina, leading to nonlinear optokinetic responses.^{21,29,38} Saturation also occurs in the central integration processes of vestibular afferents leading to a decrease in VOR performance at velocities higher than 120 degrees per second.^{30,31,33} We were careful to choose small (component) amplitudes in an attempt to avoid saturation. Furthermore, we did not encounter any significant distortion products in the CEM conditions tested. This is a key feature of saturation, as it prominently changes the shape of the signal, and hence its frequency content. Additionally, we see no change in a quantitative measure of distortion in the OKR with increasing frequency (and therefore velocity). Nonetheless, saturation cannot be fully excluded, as distortion products are typically small, and thus hard to detect in relatively noisy eye velocity signals. Most of the data presented here are recorded at an amplitude of 2 degrees. This 2 degree amplitude does increase the velocity of the signals and thus a greater possibility for saturation of the velocity sensitive retinal neurons to explain the nonlinearities. Our experiments also included a 1 degree testing condition and we do still see the presence of nonlinearities. The pattern of nonlinearities reported for the 2 degree condition are still present in the 1 degree condition as can be seen from Figure 7. In each case, the diamond and circle, representing 2 degrees and 1 degree, respectively, always lie on the same side of the line of identity and never on it. Points lying on the line represent a linear system and deviations from this are consistently represented in both amplitude conditions. The occurrence of the same pattern of nonlinearities at velocities that are half of those of the 2 degree condition argues against a simple velocity saturation. Combination of stimuli may still dramatically increase the peak velocity of the signal, hence we do not discount the possibility that there may be some OKR saturation present to explain our nonlinearities. However, if indeed the nonlinearities represented by

the relative gains of the OKR and SVOR may be explained by saturation that is undetectable in our dataset, the nonlinearities represented in the relative delays of the VOR and VVOR would appear to stem from a different source. Given the velocity saturation of the vestibular system at very high velocities, it could be claimed that the nonlinear relative delay is a consequence of this; however, the value of 120 degrees per second is more than double the velocity of our highest-frequency SoS stimulus and therefore saturation would seem unlikely. Therefore, we suggest that at least two separable nonlinearities exist, one in the gain of the OKR (and consequently SVOR) and the other in the delay of the VOR (and consequently the VVOR).

We see our work as a key first step in the application of more complex stimuli to challenge our understanding of how the CEM works. The current picture that emerges of CEM function from simple stimuli can be highly misleading given the predictable nature of SS stimuli. If we want to extrapolate how the CEM system will react to novel stimuli, as seen in daily situations, we must make certain it has been tested in a rich enough environment. Sum of sine stimulation may still be quite simple, but it is sufficient to expose the limitations of the linear approach to the nonlinear oculomotor system. If indeed the response to a single sine wave is the result of a reflexive and a prediction signal, whereas this prediction is absent in more complex stimuli, a paradox occurs. Despite the simplicity of an SS wave, the response is actually more complicated.

Acknowledgments

Supported by the C7 Marie Curie ITN initiative (TS, PH), TC2N Interreg Grant (OD, MF), and a Postdoctoral Fellowship from the Kreitman School for Advanced Studies at BGU (PH).

Disclosure: **T.M. Sibindi**, None; **P.J. Holland**, None; **J.N. van der Geest**, None; **O. Donchin**, None; **M.A. Frens**, None

References

1. Delgado-García JM. Why move the eyes if we can move the head? *Brain Res Bull.* 2000;52:475–482.
2. Stamper SA, Roth E, Cowan NJ, Fortune ES. Active sensing via movement shapes spatiotemporal patterns of sensory feedback. *J Exp Biol.* 2012;215:1567–1574.
3. Nelson ME, MacIver MA. Sensory acquisition in active sensing systems. *J Comp Physiol A Neuroethol Sens Neural Behav Physiol.* 2006;192:573–586.
4. Hirata Y, Highstein SM. Acute adaptation of the vestibuloocular reflex: signal processing by floccular and ventral parafloccular Purkinje cells. *J Neurophysiol.* 2001;85:2267–2288.
5. Blazquez P, Hirata Y, Heiney S, Green A, Highstein S. Cerebellar signatures of vestibulo-ocular reflex motor learning. *J Neurosci.* 2003;23:9742–9751.
6. Collewijn H. Optokinetic eye movements in the rabbit: input-output relations. *Vision Res.* 1969;9:117–132.
7. Barnes GR. Visual-vestibular interaction in the control of head and eye movement: the role of visual feedback and predictive mechanisms. *Prog Neurobiol.* 1993;41:435–472.
8. Oppenheim AV, Schaffer RW. *Discrete-Time Signal Processing.* Englewood Cliffs, NJ: Prentice Hall. 1989:18–25.
9. Robinson DA. The use of control systems analysis in the neurophysiology of eye movements. *Annu Rev Neurosci.* 1981;4:463–503.
10. Kawato M, Gomi H. The cerebellum and VOR/OKR learning models. *Trends Neurosci.* 1992;15:445–453.
11. Schonewille M, Luo C, Ruigrok TJH, et al. Zonal organization of the mouse flocculus: physiology, input, and output. *J Comp Neurol.* 2006;497:670–682.

12. Kimpo RR, Raymond JL. Impaired motor learning in the vestibulo-ocular reflex in mice with multiple climbing fiber input to cerebellar Purkinje cells. *J Neurosci.* 2007;27:5672-5682.
13. Lisberger SG, Miles FA, Optican LM. Frequency-selective adaptation: evidence for channels in the vestibulo-ocular reflex? *J Neurosci.* 1983;3:1234-1244.
14. Barmack NH, Yakhnitsa V. Functions of interneurons in mouse cerebellum. *J Neurosci.* 2008;28:1140-1152.
15. Frens MA, Mathoera AL, Van Der Steen J. Floccular complex spike response to transparent retinal slip. *Neuron.* 2001;30:795-801.
16. De Zeeuw CI, Wylie DR, Stahl JS, Simpson JI. Phase relations of Purkinje cells in the rabbit flocculus during compensatory eye movements. *J Neurophysiol.* 1995;74:2051-2064.
17. Winkelman B, Frens M. Motor coding in floccular climbing fibers. *J Neurophysiol.* 2006;95:2342-2351.
18. Simpson JI, Belton T, Suh M, Winkelman B. Complex spike activity in the flocculus signals more than the eye can see. *Ann N Y Acad Sci.* 2002;978:232-236.
19. Massot C, Chacron MJ, Cullen KE. Information transmission and detection thresholds in the vestibular nuclei: single neurons vs. population encoding. *J Neurophysiol.* 2011;105:1798-1814.
20. Massot C, Schneider AD, Chacron MJ, Cullen KE. The vestibular system implements a linear-nonlinear transformation in order to encode self-motion. *PLoS Biol.* 2012;10:e1001365.
21. van Alphen B, Winkelman BHJ, Frens MA. Three-dimensional optokinetic eye movements in the C57BL/6J mouse. *Invest Ophthalmol Vis Sci.* 2010;51:623-630.
22. Frens MA, Mathoera AL, Van Der Steen J. On the nature of gain changes of the optokinetic reflex. *Prog Brain Res.* 2000;124:247-255.
23. Collewijn H. The vestibulo-ocular reflex: an outdated concept? *Prog Brain Res.* 1989;80:197-209.
24. Badura A, Schonewille M, Voges K, et al. Climbing fiber input shapes reciprocity of Purkinje cell firing. *Neuron.* 2013;78:700-713.
25. Cullen KE, Roy JE. Signal processing in the vestibular system during active versus passive head movements. *J Neurophysiol.* 2004;91:1919-1933.
26. van der Heijden M, Joris PX. Panoramic measurements of the apex of the cochlea. *J Neurosci.* 2006;26:11462-11473.
27. Meenderink SWF, van der Heijden M. Distortion product otoacoustic emissions evoked by tone complexes. *J Assoc Res Otolaryngol.* 2010;12:29-44.
28. Iwashita M, Kanai R, Funabiki K, Matsuda K, Hirano T. Dynamic properties, interactions and adaptive modifications of vestibulo-ocular reflex and optokinetic response in mice. *Neurosci Res.* 2001;39:299-311.
29. van Alphen AM, Stahl JS, De Zeeuw CI. The dynamic characteristics of the mouse horizontal vestibulo-ocular and optokinetic response. *Brain Res.* 2001;890:296-305.
30. Dow ER, Anastasio TJ. Violation of superposition by the vestibulo-ocular reflex of the goldfish. *Neuroreport.* 1996;7:1305-1309.
31. Sudlow LC, Anastasio TJ. Violation of homogeneity by the vestibulo-ocular reflex of the goldfish. *Neuroreport.* 1999;10:3881-3885.
32. Minor LB, Lasker DM, Backous DD, Hullar TE. Horizontal vestibuloocular reflex evoked by high-acceleration rotations in the squirrel monkey. I. Normal responses. *J Neurophysiol.* 1999;82:1254-1270.
33. Paige GD. Vestibuloocular reflex and its interactions with visual following mechanisms in the squirrel monkey. I. Response characteristics in normal animals. *J Neurophysiol.* 1983;49:134-151.
34. Frens MA, Donchin O. Forward models and state estimation in compensatory eye movements. *Front Cell Neurosci.* 2009;3:13.
35. Roth E, Zhuang K, Stamper SA, Fortune ES, Cowan NJ. Stimulus predictability mediates a switch in locomotor smooth pursuit performance for *Eigenmannia virescens*. *J Exp Biol.* 2011;214:1170-1180.
36. Lisberger SG. Internal models of eye movement in the floccular complex of the monkey cerebellum. *Neuroscience.* 2009;162:763-776.
37. Winkelman BHJ, Belton T, Suh M, Coesmans M, Morpurgo MM, Simpson JI. Nonvisual complex spike signals in the rabbit cerebellar flocculus. *J Neurosci.* 2014;34:3218-3230.
38. Collewijn H. Changes in visual evoked responses during the fast phase of optokinetic nystagmus in the rabbit. *Vision Res.* 1969;9:803-814.